J Mater Sci (2008) 43:652–659
DOI 10.1007/s10853-007-2155-z

Freeze cast carbon nanotube-alumina nanoparticle green composites

Kathy Lu

Received: 12 June 2007 / Accepted: 10 September 2007 / Published online: 17 October 2007

Abstract CNT-Al_2O_3 nanoparticle suspensions without and with sodium dodecyl sulfate (SDS) were freeze-cast into green samples. SDS drastically improves Carbon nanotube (CNT) dispersion and CNT-Al_2O_3 nanocomposite homogeneity. Green density of the CNT-Al_2O_3 nanocomposites decreases with CNT addition. Green strength of the CNT-Al_2O_3 nanocomposites increases with the CNT content when CNTs are well separated. The CNT-Al_2O_3 nanocomposites show medium energy fracture mode during equibiaxial flexural strength testing and change color in response to CNT content and distribution in the Al_2O_3 nanoparticle matrix.

Introduction

Carbon nanotubes (CNTs) have up to 300 m^2/g specific surface area, greater than 65 GPa tensile strength, greater than 1,000 GPa modulus of elasticity, 10–30% elongation, and 2,000 W/mK thermal conductivity [1–3], all at less than 50% of the weight of Al_2O_3. When introduced into ceramic matrix, CNTs have the potential of drastically improving the composite mechanical properties [4, 5]. For example, the average bending strength and fracture toughness of CNT-SiO_2 composite were enhanced by 88% and 146% respectively compared with monolithic SiO_2 glass [6]. Crack deflection, crack bridging, and CNT pull-out toughening mechanisms were reported to operate in CNT reinforced Al_2O_3 composites [7]. More importantly, CNT-ceramic composites can be tailored for electrical conductivity. For CNT-spinel composite made by a CCVD route, 11 vol% CNTs was reported to be the percolation threshold for conductivity [8]. Other studies by conventional mixing and pressure sintering reported similar results [9, 10]. CNT-metal oxide (such as Al_2O_3, MgO) nanocomposites were extruded at high temperatures. The CNTs withstood the extreme shear stresses occurring during the extrusion. The materials showed electrical conductivity anisotropy, which could be adjusted by controlling the amount of CNTs [11]. These unique properties present exciting possibilities of engineering CNT-Al_2O_3 nanocomposites. Potential applications for CNT-Al_2O_3 nanocomposites range from high strength, lightweight structural components, electrostatic dissipation units, to thermal shock resistant components.

However, two issues have to be addressed for CNT-Al_2O_3 nanocomposite processing. First, CNT dispersion should be improved in order to realize the predicted benefit of adding CNTs into the Al_2O_3 matrix at the optimal amount. The immense surface area of CNTs has been a barrier for uniform CNT dispersion. In the above studies, the CNT content is substantially higher than the pure CNT dispersion percolation threshold [1]. Second, it is very challenging to form high green density Al_2O_3 nanoparticle compacts. The large frictional force between the nanoparticles makes dry compaction impractical, especially when homogeneous microstructure is desired. Colloidal processing that can enable high nanoparticle solids loading is the only viable approach for homogeneous and high green density microstructures. Additionally, the impact of dispersing CNTs in the Al_2O_3 matrix on the green compact density and strength need to be studied. CNT-Al_2O_3 mixture was produced and pressure sintered but the CNT dispersion was not optimized [9, 12, 13].

K. Lu (✉)
Department of Materials Science and Engineering, Virginia Polytechnic Institute and State University, 211B Holden Hall-M/C 0237, Blacksburg, VA 24061, USA
e-mail: klu@vt.edu

Freeze casting is a process that pours suspension into a nonporous mold, freezes the suspension, demolds the component, and then dries the component under vacuum. Very desirably, freeze casting has the advantages of forming near-net-shape complex geometry parts with low pressure and often environmentallybenign advantages [14, 15]. When the freeze casting condition is properly controlled, water separates from the solid phases through sublimation and there is no capillary force to cause cracks [16, 17]. Freeze casting has great potential of maintaining the uniform dispersion of equiaxed Al_2O_3 nanoparticles and large aspect ratio CNTs from the suspension state. However, so far the studies are either focused on micron size particles or metal-organic salt sol-gel systems [18–20]. Only our recent efforts involve forming high green density Al_2O_3 nanoparticle compacts by freeze casting [21–23].

In this study, two different approaches of dispersing multi-walled CNTs and Al_2O_3 nanoparticles are studied. One is using poly(acrylic acid) (PAA) as dispersant for the CNT-Al_2O_3 suspension. The other is using sodium dodecyl sulfate (SDS) to improve CNT dispersion first before adding PAA and Al_2O_3 nanoparticles to the suspension. After that, the CNT-Al_2O_3 nanoparticle suspensions are freeze-cast into green samples. The microstructural homogeneity of the freeze-cast samples is compared, the green sample densities and equibiaxial strength are measured, and the green sample fracture mode and color are evaluated. CNT distribution has clear impact on the green density and strength, which are discussed in correlation with the microstructures of the freeze-cast samples.

Experimental procedure

Al_2O_3 nanoparticles with specific surface area of 45 m^2/g were used in this study (Nanophase Technologies, Romeoville, IL). The particle size distribution measurement from dynamic light scattering (number-based) is shown in Fig. 1 (Zetasizer Nano ZS, Malvern Instruments, Inc., Southborough, MA). The CNTs used were produced by chemical vapor deposition and briefly acid-treated for purification (Helix Material Solutions, Richardson, TX). These are multi-walled CNTs with 10–30 nm diameter, 0.5–40 μm length, and 300 m^2/g specific surface area. A SEM image of the CNTs is shown in Fig. 2.

Aqueous CNT suspensions showed that at >0.5 vol% CNT contents, the viscosity of the CNT dispersion dramatically increased. At 4.0 vol%, the system was able to support its own weight as a freestanding gel [1]. In our prior work, 40 vol% solids loading CNT-Al_2O_3 nanoparticle co-dispersions of 0, 0.14, 0.27, 0.5, 1.3, and 2.6 vol% CNT contents were prepared. CNT content of ≥1.3 vol% showed substantial viscosity increase and was deemed unsuitable for freeze casting process [24]. Based on this knowledge, the CNT content in this work was varied at 0, 0.14, 0.27, 0.5, and 0.8 vol% of the whole suspension system. It should be mentioned that these low CNT contents are in sharp contrast with the high CNT contents used for other processes [5, 8–10]. This is because the conventional processes lack the ability of uniformly dispersing CNTs. There is an 'over-use' of CNTs that has not been addressed. Also, the impact of uniform CNT dispersion on colloidal suspension flowability is significant, as demonstrated in our work and others [6, 24–26]. But such issue is absent in the above conventional studies.

For effective dispersion of CNTs in the CNT-Al_2O_3 nanoparticle suspension, the surface charges of CNTs and Al_2O_3 nanoparticles at different pH were evaluated by zeta-potential measurements (Zetasizer Nano ZS, Malvern Instruments, Inc., Southborough, MA). For the as-received CNTs and SDS ($C_{12}H_{25}OSO_3Na$, 99%, Fisher Scientific, Fair Lawn, NJ) dispersed CNTs, a fixed amount was milled in water for 12 h and the zeta-potential was measured. Ten zeta-potential values from the zeta-potential analyzer were averaged and reported for each suspension.

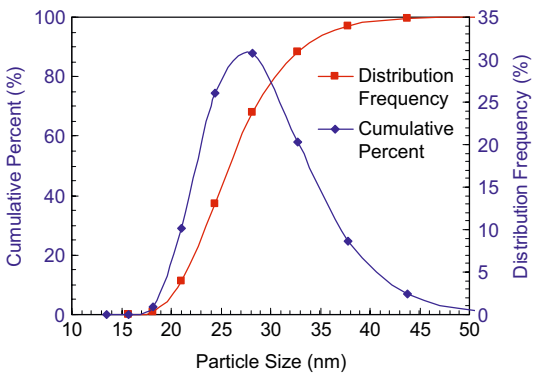

Fig. 1 Al_2O_3 nanoparticle size distribution

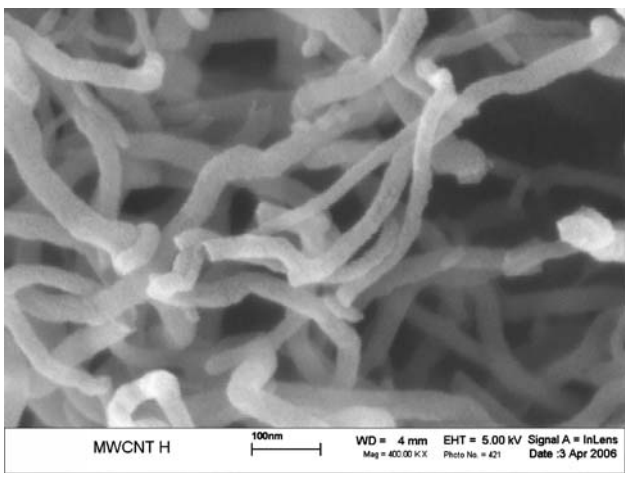

Fig. 2 SEM image of the multi-walled CNTs used in the study

For the preparation of the CNT-Al_2O_3 suspensions, PAA (M_W 1,800, Aldrich, St Louis, MO) was used as dispersant. PAA has monomer segment as [-$CH_2CH(CO_2H)$-]. Glycerol ($C_3H_8O_3$, water basis, Fisher Chemicals, Fairlawn, NJ) was used to lower the freezing temperature of the suspension and refine the ice microstructure for homogeneous component formation during freeze casting. Theoretically, glycerol binds to water molecules and disrupts the complete crystallization of ice, resulting in a localized amorphous structure, thus reducing the size of the growing ice crystal and inhibiting particle rejection [19]. Water:glycerol ratio of 9:1 was used for the dispersing medium, which was homogenized for 5 min using a ball mill before any solid phase was dispersed. For the CNT-Al_2O_3 suspension using PAA only, Al_2O_3 nanoparticles were added into the water–glycerol dispersing medium to achieve 20 vol% solids loading in 10 g increments along with PAA dispersant at 2 wt% of Al_2O_3. Since low pH promotes PAA dispersant adsorption onto the Al_2O_3 nanoparticles [27], HCl solution was added into the Al_2O_3 suspension to lower the pH to 1.5 for PAA adsorption. After these steps, the pH of the suspension was adjusted to 9.5. CNTs were weighed and added in 100 mg increments into the 20 vol% Al_2O_3 suspension at pH 9.5, followed by ball milling homogenization for 1 h after each 100 mg CNT addition. After the CNT addition, more Al_2O_3 nanoparticles were added into the suspension in 10 g increments, along with more PAA addition to maintain the overall content of 2.0 wt% Al_2O_3 and the adjustment of the suspension pH to 9.5. By this method, 40 vol% solids loading CNT-Al_2O_3 suspensions were prepared. For the CNT-Al_2O_3 suspensions using PAA and SDS, CNTs of the above-targeted ratios for the final suspensions were dispersed first using SDS in the 9:1 water–glycerol dispersing medium. SDS content was 4.0 mM of the dispersing medium amount as to be discussed next. PAA and Al_2O_3 were then added into the CNT containing dispersing medium at pH 1.5 followed by homogenization to form 20 vol% solids loading suspension with PAA at 2 wt% of Al_2O_3. After that, the 40 vol% solids loading CNT-Al_2O_3 suspensions were prepared in the same manner as the CNT-Al_2O_3 suspensions without SDS.

For the CNT-Al_2O_3 suspension freeze casting, freeze-cast molds of 25.40 mm diameter and 1.58 mm thickness were made using poly(dimethyl siloxane) polymer (RTV 664, GE, Waterford, NY). The stabilized suspension was placed into the mold cavities using a disposable plastic pipette. Care was taken to completely fill the molds with the CNT-Al_2O_3 suspension to prevent large air bubbles. After the mold filling, the samples were allowed to rest for 1 h and then frozen at –35 °C for 2 h. The frozen samples were then removed from the molds and placed back into the freeze dryer. The freeze dryer chamber was evacuated to $<10^3$ Pa pressure for 36 h to sublimate ice.

Green density of the freeze-cast samples was measured by measuring the weight and dimensions of a given sample. The organic content was deducted from green density calculation and the density results represent the packing density of Al_2O_3 nanoparticles and CNTs only.

Equibiaxial flexural strength of the freeze-cast CNT-Al_2O_3 samples was determined following ASTM C 1499 [28]. The samples were tested using a texture analyzer test console equipped with a 5 kN load cell (Stable Micro Systems, Surrey, UK). A schematic of the setup is shown in Fig. 3. When a sample was aligned in the test fixture, caution was taken to ensure that the load ring and the support ring were concentric. To ensure point loading, a ball bearing was placed in the load fixture. The console was set to record compressive force and the crosshead was lowered monotonically at a speed of 0.1 mm/min. The shape of the force versus displacement curve was recorded. The sample fracture mode was examined for each CNT-Al_2O_3 composition. The fracture surface for different CNT-Al_2O_3 composites was examined by a scanning electron microscopy (Carl Zeiss MicroImaging, Inc., Thornwood, NY) to ensure that the fracture mode conformed to a valid fracture per ASTM C 1499. The fractured sample was measured with a digital micrometer to determine the exact thickness at the most likely crack initiation point. The equibiaxial flexural strength was then calculated for each sample, using the following equation:

$$\sigma_f = \frac{3F}{2\pi h^2}\left[(1-\nu)\frac{D_S^2 - D_L^2}{2D^2} + (1+\nu)\ln\frac{D_S}{D_L}\right] \quad (1)$$

where σ_f is fracture strength in MPa, F is breaking load in N, h is specimen thickness in mm, ν is Poisson's ratio, D is sample diameter in mm, D_S is support ring diameter in mm, and D_L is load ring diameter in mm.

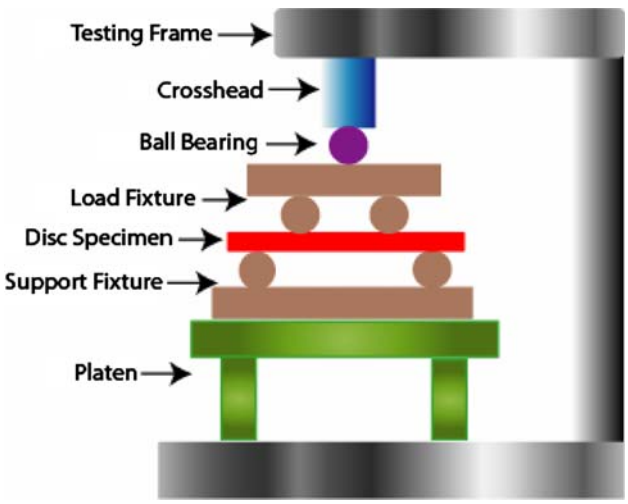

Fig. 3 Cross-section view of equibiaxial flexural strength test apparatus, after ASTM C 1499 [28]

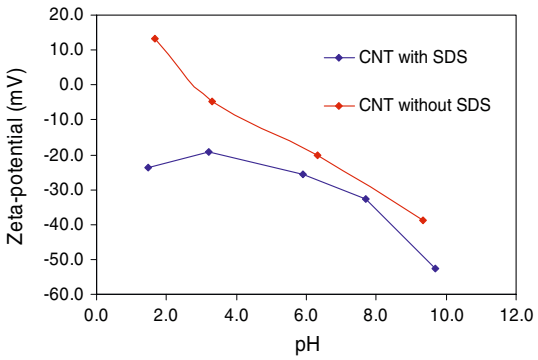

Fig. 4 CNT dispersion zeta-potential variation versus pH without SDS and with SDS

Results and discussion

Colloidal interactions of CNTs and Al_2O_3 nanoparticles

As shown in Fig. 4, pure CNTs have positive zeta-potential at pH < 2.8. At pH 9.5, the CNTs have <–30 mV zeta-potential. This zeta-potential characteristic is different from that of concentrated nitric acid and sulfuric acid treated CNTs [29], which have <–25 mV zeta potential from pH 2–12. Nevertheless, at pH 9.5 CNTs should repel from Al_2O_3 nanoparticles, which have –41 mV zeta potential from the adsorbed PAA dispersant [21, 30, 31]. However, freeze-cast sample microstructure shows that CNTs are not uniformly dispersed as to be discussed. The observation indicates that two conditions have to be met for good CNT dispersion in the Al_2O_3 matrix. The first is the effective dispersion of CNTs themselves and the second is the uniform distribution of CNTs in-between the Al_2O_3 nanoparticles. Without deliberate CNT separation, the first condition is not met. For CNTs to separate from each other and uniformly disperse in-between the Al_2O_3 nanoparticles, a suitable dispersant needs to be used, which should attach to the CNT surface for improved CNT separation. Also, the dispersant should provide negative zeta potential as PAA stabilized Al_2O_3 does. Since SDS is anionic, similar to PAA, and has the hydrophobic carbon chain on the other end to adsorb onto CNTs, dispersing CNTs by SDS shows to be an effective approach (Fig. 4). With SDS, CNTs have negative zeta potential (–20 mV or less) at all pH conditions, consistent with other work reported [32].

Preliminary CNT dispersion quality can be evaluated by optical microscopy. If aggregates are observed, it indicates poor CNT separation. If aggregates are not observed, it indicates much improved CNT separation. For the CNTs dispersed in water without and with SDS, the results are shown in Fig. 5. The dispersion without SDS (Fig. 5(a)) shows large aggregates of CNTs (dark flocs) in the water–glycerol medium (light background). The dispersion with

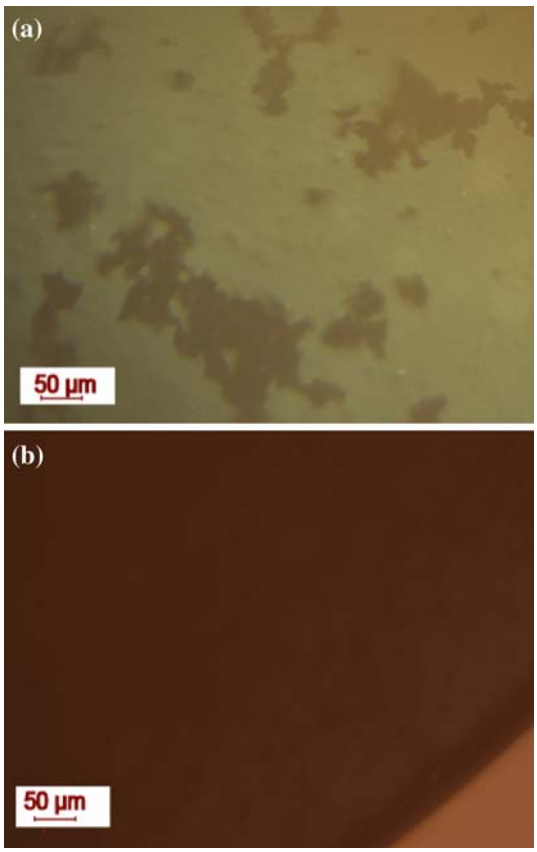

Fig. 5 CNT dispersion effectiveness comparison: (**a**) without SDS, (**b**) with SDS

SDS (Fig. 5(b)) shows no aggregates of CNTs. Homogeneous CNT dispersion with SDS leads to uniform dark color of CNTs in the water–glycerol medium. The optimal SDS concentration has been evaluated based on the critical micelle concentration of SDS in water, at 8.0 mM [33, 34]. As shown in Fig. 6, SDS dispersed CNT suspension has many air bubbles at critical micelle concentration of 8.0 mM, a phenomenon extremely undesirable for freeze casting process pore removal. This is because fundamentally SDS is also a surfactant, which has a tendency for bubble generation. At 50% of critical micelle concentration, 4.0 mM, air bubbles are substantially reduced with no compromise on CNT dispersion. According to these observations, CNTs are dispersed with 4.0 mM SDS (based on dispersing medium volume) before mixing with Al_2O_3 nanoparticles.

CNT distribution in Al_2O_3 nanoparticle matrix

For the CNT-Al_2O_3 nanoparticle samples without SDS, CNTs are not well dispersed in the Al_2O_3 nanoparticle matrix. Agglomerates of CNTs can be easily found in the fractured surface. For the CNT-Al_2O_3 nanoparticle samples

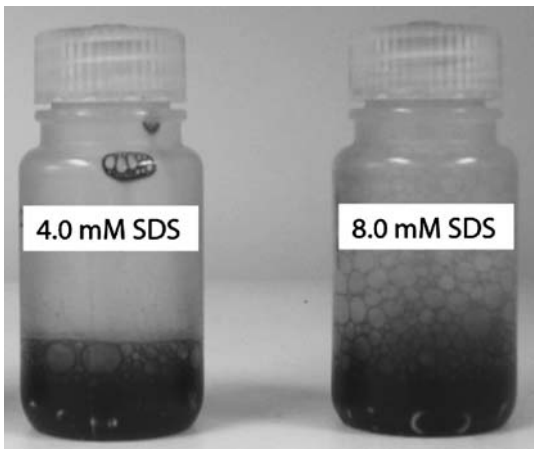

Fig. 6 SDS concentration effect on CNT dispersion and bubble formation. The white color at the bottom of the container is alumina-milling media

with SDS, uniform CNT distribution is observed. As an example, SEM images of the fracture surfaces of 0.5 vol% CNT-Al_2O_3 freeze-cast samples are shown in Fig. 7. Figure 7(a) is the sample without SDS and Fig. 7(b) is the sample with SDS. CNT distribution homogeneity difference can be clearly observed. The freeze-cast CNT-Al_2O_3 samples at 0.14 vol%, 0.27 vol%, and 0.8 vol% CNTs show the same trend. Since Al_2O_3 and CNTs have the same negative zeta-potential in the suspension and should separate from each other, the agglomerated CNTs must come from the poor CNT dispersion before Al_2O_3 nanoparticles are added. Effective CNT dispersion before the Al_2O_3 nanoparticles are introduced into the suspension is the key in realizing the projected performance improvement in CNT-Al_2O_3 nanocomposites. SDS proves to be an effective choice for the studied system.

CNT-Al_2O_3 nanocomposite green density

Since the freeze-cast samples do not have perfectly flat surface, small variation in the sample thickness introduces density measurement errors. It is difficult to quantify the density difference for the CNT-Al_2O_3 composites without and with SDS. With this knowledge, the green densities of the freeze-cast CNT-Al_2O_3 composites without SDS at different CNT vol% are shown in Fig. 8. At 0 vol% CNTs, the freeze-cast green densities range from 49% to 55%. For Al_2O_3 nanoparticle green samples, this is a fairly high green density level. Even for dry compaction process, this density can be difficult to achieve because of the large frictional force among the nanoparticles. This shows freeze casting is a promising approach to overcoming the Al_2O_3 nanoparticle poor packing issue for forming purposes.

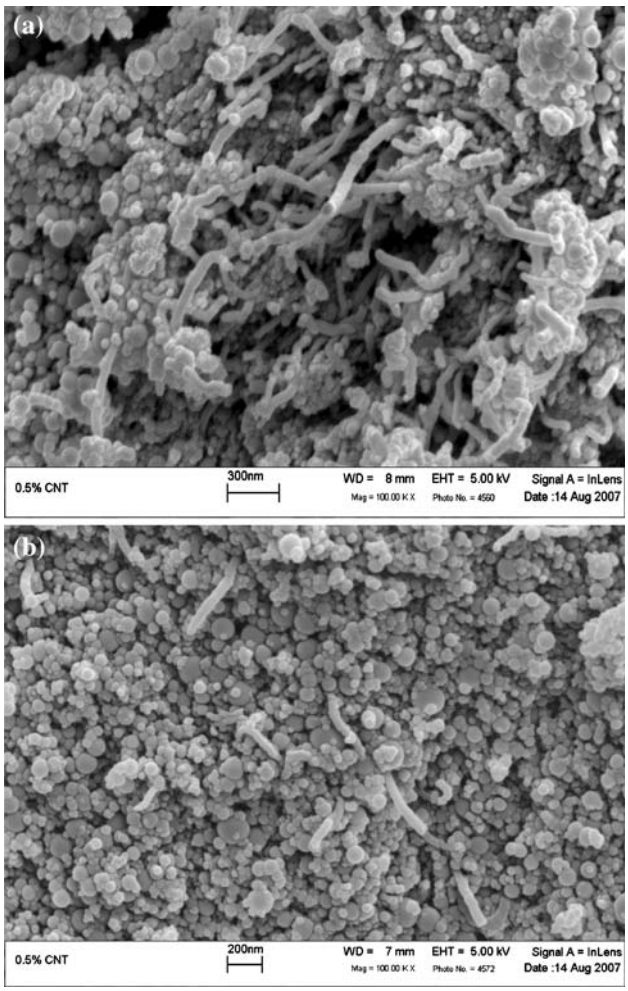

Fig. 7 SEM images of freeze-cast microstructures: (**a**) without SDS, (**b**) with SDS

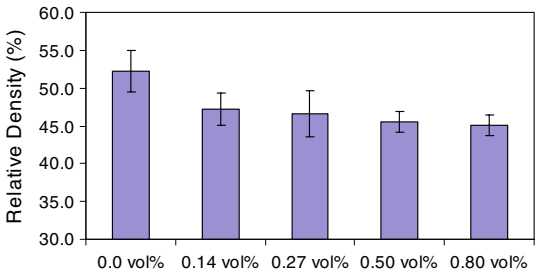

Fig. 8 Densities of CNT-Al_2O_3 nanoparticle composites at different CNT contents

The CNT-Al_2O_3 composites at all CNT levels have lower densities than the pure Al_2O_3 nanoparticle sample does, varying between 44 and 49 vol%. The density decrease is apparently caused by CNT addition since all the other variables are kept the same. The CNT-Al_2O_3 nanoparticle composite can be envisioned as a mixture of glass beads (corresponding to Al_2O_3 nanoparticles) and fibers (corresponding to CNTs). During freeze casting, the CNTs

themselves are separated, less effectively without SDS and more effectively with SDS. Since CNTs are distributed among the Al_2O_3 nanoparticles, they are likely to disrupt the Al_2O_3 nanoparticle close packing and decrease the CNT-Al_2O_3 composite green density. In light that the CNT vol% is very low in comparison to Al_2O_3 vol%, it is difficult to differentiate the impact of increasing CNT vol%. This observation indicates the adverse impact of CNTs in achieving high green density for the CNT-Al_2O_3 nanocomposites. During further densification (such as sintering), the effect of CNTs should be closely examined in order to realize the expected performance improvement.

Equibiaxial flexural strength evaluation

The equibiaxial flexural strength of the freeze-cast samples was calculated via Eq. 1. The equibiaxial flexural strength test can be considered as a four-point bending test with 360° rotation about the load axis. Hence, it has the advantage of isotropic testing conditions, whereas the four-point bending test exerts high stress in the direction perpendicular to its supports. The equibiaxial flexural strength test was conceived to eliminate the effect of edge (corner) defects that result from the shape of a bar test specimen [35]. In this study, all the samples are examined to ensure that they conform to a valid fracture mode, per specification. Any samples in which the cracks appear to have initiated outside of the load ring are deemed invalid.

Average green strength values for the CNT-Al_2O_3 nanoparticle samples at different CNT contents without and with SDS are shown in Fig. 9. Poisson's ratio v is assumed to be 0.2. A deviation of $\sim$25% in the Poisson's ratio results in approximately 2% change in the equibiaxial flexural strength and the calculation is made with this knowledge. It should also be mentioned that the starting Al_2O_3 nanoparticles from different batches greatly affect the green strength. The main cause is nanoparticle zeta-potential variation which requires different optimal suspension preparation conditions. The results in Fig. 9 are obtained with the same batch Al_2O_3 nanoparticles and under the same suspension preparation conditions.

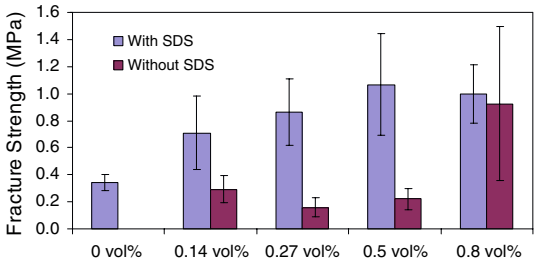

Fig. 9 Equibiaxial flexural strength of freeze-cast CNT-Al_2O_3 samples without and with SDS

As Fig. 9 shows, Al_2O_3 nanoparticle samples with 0 vol% CNTs have 0.34 ± 0.05 MPa strength. Even though it is fairly low compared to that of fully dense samples, the strength is high enough for post-freeze casting handling and sintering densification purposes. For the CNT-Al_2O_3 nanoparticle samples, the strength results show two trends. For the CNT-Al_2O_3 samples without SDS, the green strength stays the same or decreases with CNT addition up to 0.5 vol% CNTs. With further CNT content increase to 0.8 vol%, the green strength increases to a higher value but with large strength scattering. For the CNT-Al_2O_3 samples with SDS, the green strength shows steady increase with CNT content, up to 0.5 vol%. After that the strength value levels off. This can be understood from three aspects. The first is the intrinsic nature of CNTs in increasing sample strength by reinforcing the Al_2O_3 matrix. The second is the CNT disruption of the close packing of Al_2O_3 nanoparticles. The third is the distribution uniformity of CNTs in the green samples. When SDS is used to disperse CNTs during the suspension preparation, CNTs distribute uniformly in the Al_2O_3 matrix and the reinforcement effectively offsets the adverse effect of disrupting Al_2O_3 nanoparticle close packing. This combinatorial effect results in higher green strength. When CNTs are introduced into the Al_2O_3 nanoparticle matrix with no SDS, poor CNT distribution plays a more significant role in disrupting Al_2O_3 nanoparticle close packing and compromising the green strength. Also, CNTs have large aspect ratio with 10–30 nm diameter, the maximum CNT vol% for discrete CNT dispersion is low when they are effectively separated. When the CNT content reaches 0.8 vol%, CNTs likely become 'connected' in the Al_2O_3 nanoparticle matrix. As a result, the benefit of adding CNTs in increasing green strength ceases to be more effective. When CNTs are dispersed without SDS, certain samples might happen to have more desired CNT dispersion to offer noticeable matrix reinforcement, leading to large green strength scattering under the same condition.

CNT-Al_2O_3 nanocomposite fracture mode and color

Examples of the fracture modes for the freeze-cast CNT-Al_2O_3 samples are shown in Fig. 10. Markers have been placed at the likely origin of the fractures. Most of the CNT-Al_2O_3 samples conform to the medium energy fracture mode [28]. The fracture edges are very smooth. It is also interesting to point out that the samples change color from white to dark blue as the CNT content increases from 0 to 0.8 vol%. This color change comes from CNT (black) addition into the Al_2O_3 nanoparticle (white) matrix. The

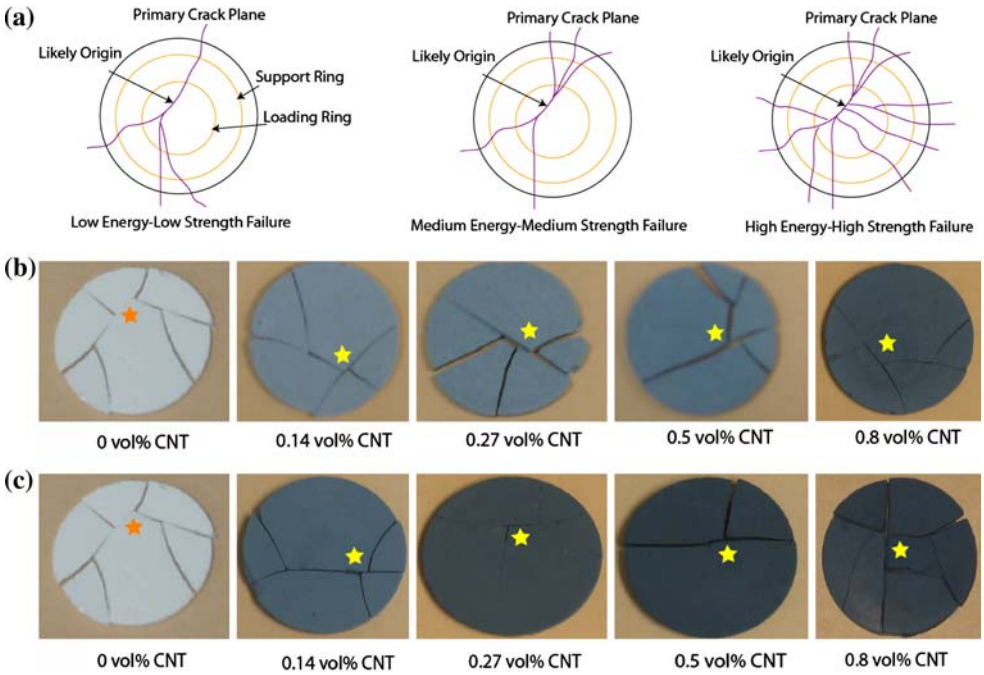

Fig. 10 Fracture mode and color change of freeze-cast CNT-Al_2O_3 samples: (**a**) different fracture modes [28], (**b**) without SDS, and (**c**) with SDS. Likely crack initiation point is indicated by a star and the original sample diameter is 25.4 mm

final color is different shades of blue depending on the CNT vol%. More importantly, there is a color difference for the samples without SDS (Fig. 10(b)) and with SDS (Fig. 10(c)). The samples with SDS show a darker color than those without SDS at all CNT contents. Since SDS enables uniform CNT dispersion, color difference directly reflects the homogeneity of the CNT distribution. When the CNTs are homogeneously distributed with SDS, the composite color is always darker under the same CNT content.

Conclusions

For the studied CNT-Al_2O_3 nanoparticle suspensions, SDS is critical in achieving uniform CNT dispersion in the Al_2O_3 nanoparticle system. Green density of the freeze-cast CNT-Al_2O_3 nanoparticle samples decreases with CNT addition. Freeze-cast green strength increases with CNT content when CNTs are well dispersed. However, there is a maximum value of $\sim$0.5 vol% CNTs for such trend. With further CNT content increase to 0.8 vol%, the CNT reinforcing effect levels off. Also, the CNT-Al_2O_3 nanocomposite shows medium energy fracture mode during the equibiaxial strength testing and the composite color change is a direct function of CNT content and CNT distribution in the CNT-Al_2O_3 nanoparticle composite.

Acknowledgements This work was supported by Oak Ridge Associated Universities and Petroleum Research Fund. The author also thanks Chris Kessler and Xiaojing Zhu for certain data collection and Prof. Brian Love for the equibiaxial flexural strength testing.

References

1. Kinloch IA, Roberts SA, Windle AH (2002) Polymer 43:7483
2. Yu M-F, Files BS, Arepalli S, Ruoff RS (2000) Phys Rev Lett 84:5552
3. Park SJ, Cho MS, Lim ST, Choi HJ, Jhon MS (2003) Macromol Rapid Commun 24:1070
4. Curtin WA, Sheldon BW (2004) Mater Today 7:44
5. Fan JP, Zhao DQ, Wu MS, Xu ZN, Song J (2006) J Am Ceram Soc 89:750
6. Ning JW, Zhang JJ, Pan YB, Guo JK (2004) Ceram Int 30:63
7. Xia Z, Riester L, Curtin WA, Li H, Sheldon BW, Liang J, Chang B, Xu JM (2004) Acta Mater 52:931
8. Rul S, Lefevre-Schlick F, Capria E, Laurent C, Peigney A (2004) Acta Mater 52:1061
9. Zhan G-D, Mukherjee AK (2004) Int J Appl Ceram Technol 1:161
10. Zhan G-D, Kuntz JD, Garay JE, Mukherjee AK (2003) Appl Phys Lett 83:1228
11. Peigney A, Flahaut E, Laurent C, Chastel F, Rousset A (2002) Chem Phys Lett 352:20
12. Fan J, Zhao D, Wu M, Xu Z, Song J (2006) J Am Ceram Soc 89:750
13. Siegel RW, Chang SK, Ash BJ, Stone J, Ajayan PM, Doremus RW, Schadler LS (2001) Scripta Mater 44:2061
14. Koch D, Andresen L, Schmedders T, Grathwohl G (2003) J Sol-Gel Sci Tech 26:149
15. Jones RW (2000) Ind Ceram 20:117
16. Bollman H (1957) Ceram Age 791:36
17. Novich BE, Sundback CA, Adams RW, (1992) In: Cima MJ (ed) Ceramic transactions, forming science and technology for ceramics, American Ceramic Society, Westerville, p 157
18. Koh Y-H, Song J-H, Lee E-J, Kim H-E (2006) J Am Ceram Soc 89:3089
19. Sofie SW, Dogan F (2001) J Am Ceram Soc 84:1459
20. Rak ZS (2000) CFI-Ceram Forum Int 77:E25
21. Lu K, Kessler CS, Davis RM (2006) J Am Ceram Soc 89:2459
22. Lu K, J Am Ceram Soc, in print

23. Lu K (2006) In: Mathur S, Laine RM, Hu MZ, Vartuli J, Koper OB (eds) Proceeding of 2006 Materials Science & Technology International Conference, American Ceramic Society, Cincinnati, p 463
24. Lu K (2007) Powder Technol 177:154
25. Sun J, Gao L (2003) Carbon 41:1063
26. Sun J, Gao L, Jin XH (2005) Ceram Int 31:893
27. Cesarano J, Aksay IA (1988) J Am Ceram Soc 71:1062
28. ASTM Designation C1499–04 (2004) American Society for Testing and Materials International, West Conshocken
29. Esumi K, Ishigami M, Nakajima A, Sawada K, Honda H (1996) Carbon 34:279
30. Lu K, Kessler CS (2006) J Mater Sci 41:5613, doi: 10.10007/s10853-006-0303-05
31. Lu K, Ceram Int, in print
32. Jiang LQ, Gao L, Sun J (2003) J Colloid Interf Sci 260:89
33. Mohamed A, Mahfoodh ASM (2006) Colloids Surf A 287:44
34. Singh G, Song LF (2006) Colloids Surf A 281:138
35. Soltesz U, Richter H, Kienzler R (1987) In: Vincenzini P (ed) High technological ceramics, Elsevier, Amsterdam, p 149